A Flexible Ultra-Thin-Body SOI Single-Photon Avalanche Diode

Pengfei Sun, Benjamin Mimoun, Edoardo Charbon and Ryoichi Ishihara

Delft University of Technology, Delft Institute of Microsystems and Nanoelectronics (DIMES)
Feldmannweg 17, 2628CT Delft, the Netherlands

Tel: +31-(0)15-2781556, Fax: +31-(0)15-2622163, Email: p.sun@tudelft.nl

Abstract

The world's first flexible ultra-thin-body SOI single-photon avalanche diode (SPAD) is reported with peak photon detection probability (PDP) at 11%, dark count rate (DCR) around 20kHz and negligible afterpulsing and cross-talk. It compares favorably with CMOS SPADs while it can be bended to 10mm-diameter and operate both in frontside- (FSI) and backside-illumination (BSI).

Introduction

Single-photon avalanche diode (SPAD) technology has been receiving wide attention for applications such as time-of-flight vision, time-correlated single-photon counting, fluorescence lifetime sensing and biomedical imaging. A SPAD is an avalanche photodiode (APD) operating above breakdown voltage, V_{BD}, in so-called Geiger mode. Due to improved CMOS fabrication, novel device structures, and new readout techniques, SPAD technology has significantly progressed in recent years [1].

Moore's Law has enabled the design of larger and larger imaging systems based on SPADs. However, current SPAD technology is generally implemented on bulk silicon and it is still difficult to realize backside-illuminated devices [2]. Furthermore, to our knowledge, no SPAD has ever been fabricated on flexible substrate, as demanded by advanced biological and life sciences research and by future medical (implantable) applications [3].

In this paper, we present the world's first flexible APD fabricated in an ultra-thin-body silicon-on-insulator (SOI) process. The APD can operate in proportional and in Geiger mode (i.e. SPAD), both in frontside- (FSI) and backside-illumination (BSI), and it is compatible with the leading organic substrates, as well as glass and quartz. The SPAD multiplication region is located in a silicon layer island with a thickness of 1.5µm, thereby enabling a photon detection probability (PDP) of 11% at 460nm. The dark count rate (DCR) is less than 20kHz at room temperature and it is dominated by band-to-band tunneling for the less dependency on temperature. Afterpulsing at a dead time longer than 1µs and cross-talk in a pitch of 10µm are negligible. After etching the substrate, the device layer on a 10µm-thick flexible polyimide was formed. The measurements refer to a device with 10µm diameter. Applications include flexible multi-aperture imaging, anti-vignetting focal plane optimization, and (implantable) bio-compatible chronic medical monitoring.

Device fabrication

The SPAD cross-section is shown in Fig. 1(a). Fabrication begins with a p-type SOI wafer prepared by epitaxy technology. To ensure good mechanical compatibility, the thickness of the top silicon layer was optimized to be 1.5µm. The N^+P junction is formed by implantation. A P^+ enhancement region is made to form the multiplication region and virtual guard ring around to prevent premature edge breakdown [4]. The Medici-simulated electric field contours are shown in Fig. 2. After junction implantation, device islands are formed by dry etching. 1.5µm TEOS PECVD oxide is deposited as insulator by two-time etch back to form a spacer at the silicon island step. Then, a 3µm physical-vapor-deposited (PVD) Al/Si(1%) is used to form anode and cathode contacts. The typical device diameter is 10µm, with different pitches (see D1 and D2).

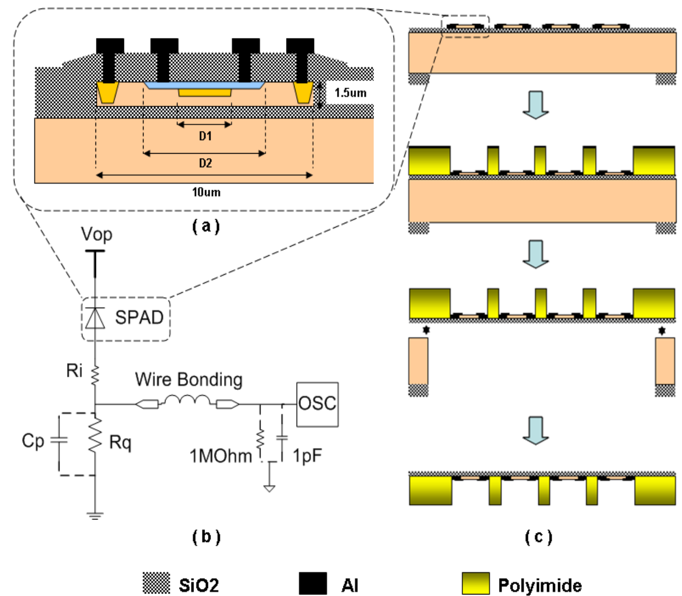

Fig.1. (a) Cross-section of device structure: D1 is the diameter of the enhancement layer, D2 is the diameter of the implicit guard ring; (b) Schematic of passive quenching circuit; (c) Transfer flow chart.

A passive quenching circuit was used in this work shown in Fig. 1(b). The anode of the SPAD with internal series resistance R_i is connected to a quenching resistance R_q of 50kOhm parallel with parasitic capacitance C_p. R_i, estimated to be around several kOhms, is due to a fully depleted area under the virtual guard ring in the 1.5 µm-thin silicon body layer. The output signal in Geiger mode is probed by oscilloscope.

The layer transfer process is summarized in Fig. 1(c). After the metallization, the polyimide is coated and cured on the top of the device at 400°C. Then, the polyimide is patterned to expose the metal contact and light absorption area. The silicon substrate under the buried oxide layer is etched away by plasma dry etching. The etching stops at the buried oxide layer and the SPAD layer on polyimide can easily be released by means of mechanical stress [5]. As a result, the SPAD's layer has been successfully transferred to flexible PEN (Polyethylene naphthalate) or other substrate. The SEM of the single device is shown in Fig. 3.

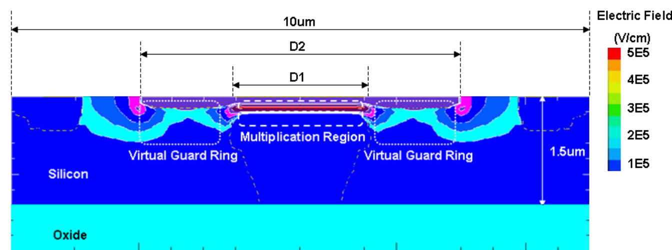

Fig. 2. 10µm-diameter SPAD device overlaid on a Medici-simulated electric field plot. In silicon, impact ionization occurs with electric fields higher than 2.5×10^5V/cm. The multiplication region is in correspondence with the enhancement layer, where the absolute value of breakdown voltage, $|V_{BD}|$, is lower. In the virtual guard ring areas, the electric field is reduced, thus preventing premature edge breakdown.

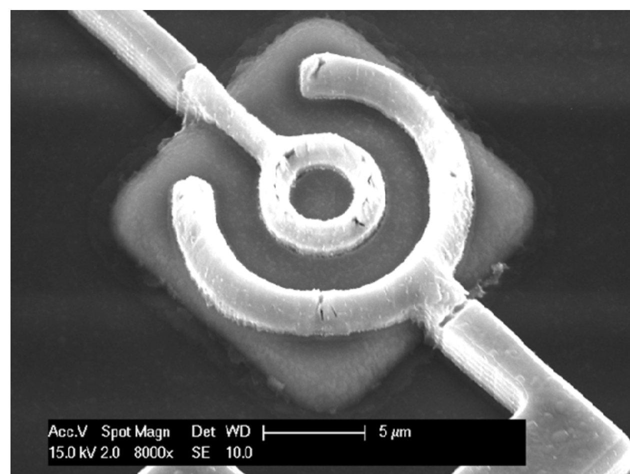

Fig.3. SEM image of an individual SOI SPAD

Measurement and analysis

The current-voltage (I-V) characteristics of the SOI SPAD are shown in Fig. 4 for different light conditions. The breakdown voltage is 12.5V.

By optimizing the dimensions of multiplication region and virtual guard ring, a DCR less than 20kHz was achieved, as shown in Fig. 5 that plots DCR as a function of excess bias voltage. The characterization of DCR as a function of temperature is shown in Fig. 6; the DCR is dominated by band-to-band tunneling instead of trap-assisted avalanching, proving the high quality of the top silicon layer.

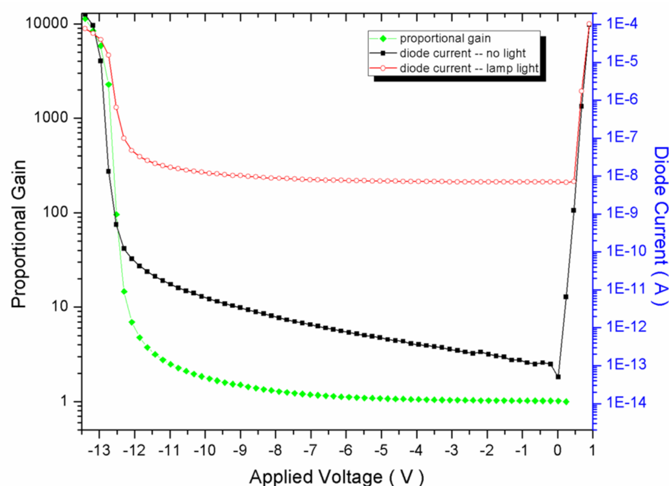

Fig. 4. I-V characteristics of SOI SPAD before transfer.

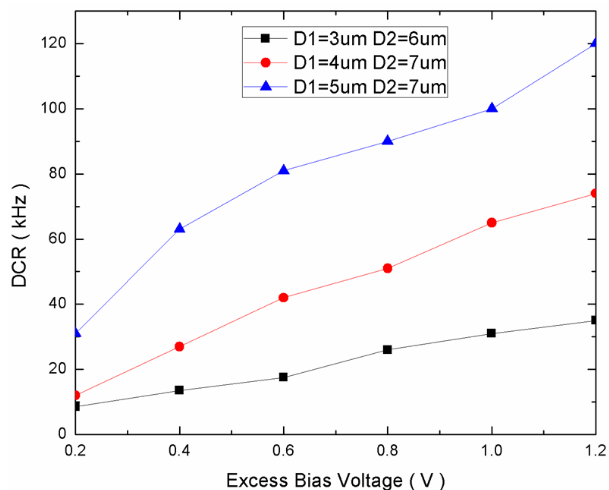

Fig. 5. Dark count rate (DCR) as a function of excess bias for different device pitch values.

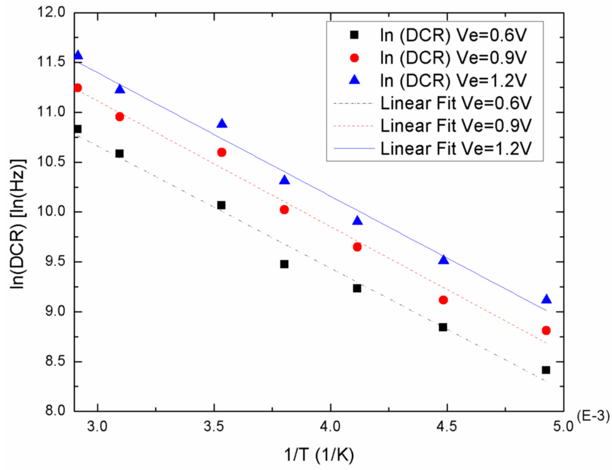

Fig. 6. DCR versus temperature at different excess bias voltages (D1=3μm, D2=6μm).

In order to characterize sensitivity, photocurrent I_d is measured at different wavelengths and compared with photocurrent I_{ref} that was measured on a reference photodiode with known quantum efficiency. The ratio I_d/I_{ref}, shown in Fig. 7, has some resonant-like peaks above 700nm, due to the cavity-like structure of the multiplication region with an interface between silicon and buried oxide similar to [6]; a similar behavior was also seen in PDP (Fig. 7), where PDP at long wavelength (700nm ~ 900nm) is enhanced. Temporal performance is shown in Fig. 8 for a 10μm-diameter SPAD with a full-width-at-half-maximum (FWHM) jitter of 500ps. The afterpulsing is characterized in Fig. 9. With a dead time longer than 1μs, the afterpulsing probability is less than 1% [7].

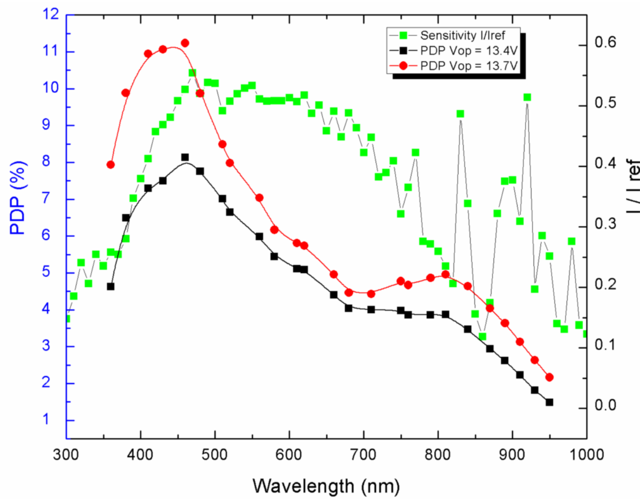

Fig. 7. Photon detection probability of the APD when operating in Geiger mode; sensitivity when operating in proportional mode as a function of wavelength (D1=5μm, D2=7μm).

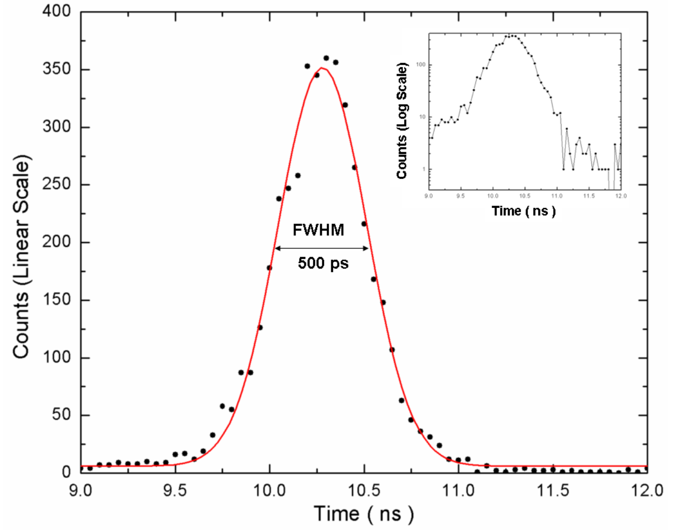

Fig. 8. Jitter performance of the APD when operating in Geiger mode (D1=5μm, D2=7μm, V_{eb}=1V).

Fig. 10 shows photographs of SPADs after being transferred onto flexible polyimide layer. The devices were re-characterized after the transfer. The measured I-V characteristics are shown in Fig. 11, where it is demonstrated that the static performance is virtually unchanged by the procedure, thus proving little impact of mechanical stress on performance.

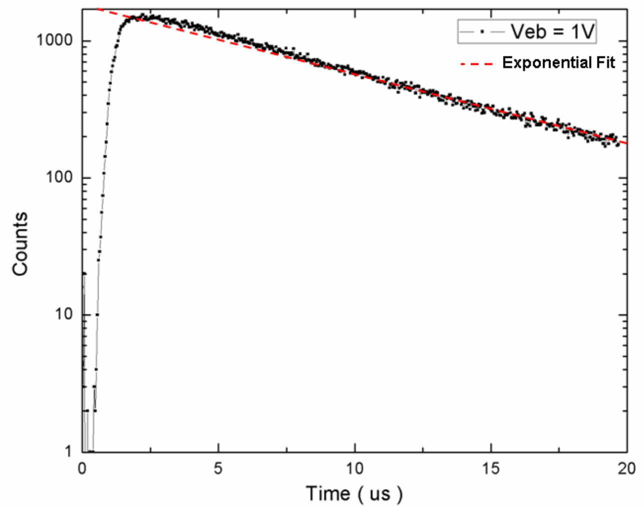

Fig. 9. Exponential fitted afterpulsing distribution at V_{eb} = 1V.

A persistent image of DCR quenching pulses of the SPAD on flexible substrate, shown in Fig.12, also proves a dead time longer than 1μs and negligible afterpulsing.

The characterization of APDs operating in proportional and Geiger mode before and after substrate transfer is summarized in Tab.1. By the comparison, the breakdown voltage and maximum DCR become a little higher after transfer. We believe that the self-heating of this behavior is when the device is encapsulated by polyimide. Over-etching through the oxide stop layer during substrate thinning may also be a

reason. PDP and time jitter show no statistically relevant changes after transfer.

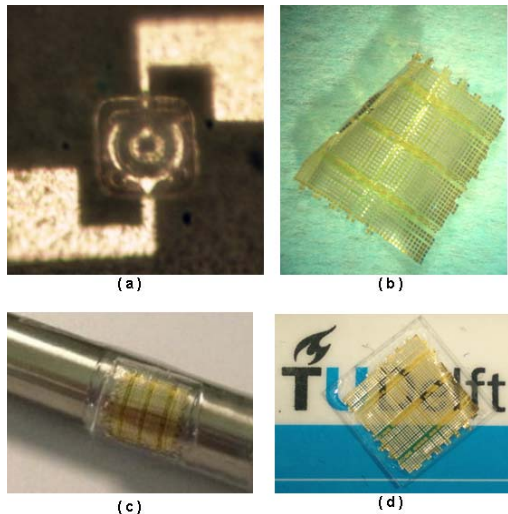

Fig. 10. (a) Microscopic picture of single SPAD on flexible substrate. (b) Flexible polyimide foil containing SPADs released from the SOI wafer. (c) Flexible SPADs on PEN substrate bent onto 10mm-diameter cylinder. (d) Flexible SPADs mounted onto quartz.

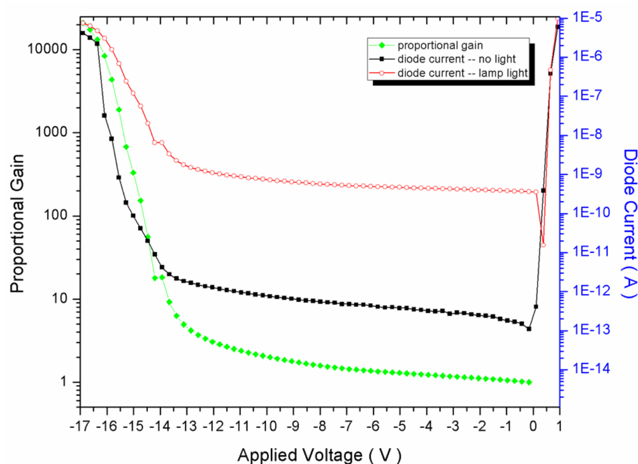

Fig. 11. I-V characteristics of SPAD transferred to flexible PEN substrate

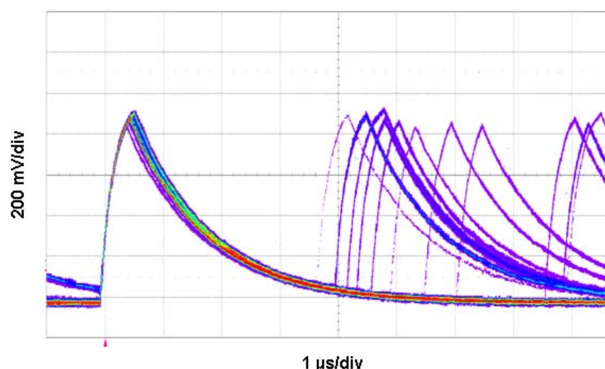

Fig. 12. Persistent image of DCR quenching pulses of SPAD after transfer.

Tab. 1. Summary of APD characterization before and after transfer.

Performance	Before Transfer			After Transfer		
	Min.	Typ.	Max.	Min.	Typ.	Max.
DCR (kHz)	20		120	20		177
V_{BD} (V) @ prop. gain=11.0		12.5			14.0	
PDP (%)			11.3			11.0
FWHM jitter (ps)		500		360		
Excess bias (V)	0		1.2	0		1.2

Conclusions

To the best of our knowledge, the reported device is the first flexible ultra-thin-body SPAD ever reported. The DCR, PDP and time jitter of the device on flexible substrate show consistency well with the performance before transfer. The device compares favorably with CMOS SPADs, while it can operate both in FSI and BSI.

Acknowledgements

The authors would like to thank all the staff of the DIMES clean rooms for processing support, especially for Mr. Michiel van der Zwan's help on transfer process, as well as Mr. Shingo Mandai and Mr. Chockalingam Veerappan from CAS for the optical and electrical measurement support.

References

[1] E. Charbon, *IEEE International Conference on Solid-State and Integrated-Circuit Technology,* 1975-1980 (2004).

[2] Nobukazu Teranishi, Hisashi Watanabe, Takehiko Ueda, and Naohisa Sengoku, *IEDM,* S24P1, 533–536 (2012).

[3] Young Ming Song, Yizhu Xie, and et. al, *Nature,* Volume: 497, 95–99 (2013).

[4] F. Zappa, S. Tisa, A. Tosi, S. Cova, *Sensors and Actuators A: Physical;* 140, (1), 103−112 (2007).

[5] B. Mimoun, V. Henneken and R. Dekker, *MRS (2010), Symposim JJ: Stretchable Electronics and Conformal Biointerfaces,* 1271E, 1271-JJ05-09 (2010).

[6] M.Ghioni, G.Armellini, P.Maccagnani, I.Rech, M.K.Emsley, and M.S. Unlu, *IEEE Photonics Technology Letters,* 20(6), 413-415 (2008).

[7] M. A.Karami, M.Gersbach, H-J. Yoon, and E. Charbon, *Optics Express,* 18(21), 22158-66 (2010).